

# A Wearable Sweat-detection Device for Inflammatory Bowel Disease Management

Group Fantastic

Department of Bioengineering  
Imperial College London

*A Project Report Submitted in  
Partial Fulfilment of the  
MEng Biomedical Engineering Degree  
MEng Molecular Bioengineering Degree*

**Supervisor:**  
Prof. Martyn Boutelle

Department of Bioengineering  
[m.boutelle@imperial.ac.uk](mailto:m.boutelle@imperial.ac.uk)

April, 2022

## **Acknowledgement**

We would like to thank Professor Martyn Boutelle for his helpful advice and supervision. We also thank Dr.Sally Gowers and Dr.Georgia Smith for their guidance in the glucose sensor fabrication, and Dr.Chiara Cicatiello for her guidance in the fabrication of the ion-selective electrode. We thank Joel Eustaquio for allocating the lab space.

# Contents

<b>1</b>	<b>Introduction</b>	<b>4</b>
1.1	Motivation . . . . .	4
1.2	Background . . . . .	4
1.2.1	Viable Biomarkers for IBD Management . . . . .	4
1.2.2	Nutrition and Hydration Status of IBD Patients . . . . .	5
1.2.3	Sweat as a Sampling Medium . . . . .	5
1.2.4	Recent Developments in Sweat-based Wearable Devices . . . . .	5
1.3	Aims & Objectives . . . . .	5
<b>2</b>	<b>Methods</b>	<b>6</b>
2.1	Material . . . . .	6
2.2	Fabrication of Needle Electrodes . . . . .	6
2.3	Preparation of Glucose Sensors . . . . .	6
2.3.1	Interference Membrane . . . . .	6
2.3.2	Enzyme Membrane . . . . .	6
2.4	Preparation of Ion-selective Electrodes . . . . .	6
2.4.1	Ion-electron Transducer . . . . .	6
2.4.2	Ion-selective Membrane . . . . .	6
2.4.3	PVB Membrane . . . . .	7
2.5	Evaluation of Sensor Performance . . . . .	7
2.5.1	Cyclic Voltammetry . . . . .	7
2.5.2	In Vitro Accuracy of Glucose Sensors . . . . .	7
2.5.3	Statistical Analysis of Glucose Sensors . . . . .	7
2.6	Signal Processing and Transmission . . . . .	7
2.6.1	Design of Processing Circuits . . . . .	7
2.6.2	Design of Arduino Circuit . . . . .	7
2.6.3	Implementation of Customized PC Program . . . . .	7
<b>3</b>	<b>Results &amp; Discussion</b>	<b>8</b>
3.1	Evaluation of Basic Functionality of Needle Electrodes . . . . .	8
3.2	Evaluation of Chlorodisation of Glucose Sensors . . . . .	8
3.3	Demonstration of Presence of Interference Membrane . . . . .	8
3.4	In Vitro Accuracy of Glucose Sensors . . . . .	8
3.5	Demonstration of Presence of Ion-electron Transducer . . . . .	8
3.6	Simulation of Processing Circuit . . . . .	9
<b>4</b>	<b>Weaknesses &amp; Opportunities</b>	<b>9</b>
<b>5</b>	<b>Conclusion</b>	<b>10</b>
<b>6</b>	<b>Extended Data</b>	<b>11</b>
<b>7</b>	<b>References</b>	<b>15</b>
7.1	Management Assessment . . . . .	17

# A Wearable Sweat-detection Device for Inflammatory Bowel Disease Management

Sophie Fretwell, Jiayi Gao, Zineb Hamdi, Zeeshan Kisat,

Weixun Luo, Daniel Muñoz, Shu Yu

May 30, 2022

## Abstract

Inflammatory Bowel Disease (IBD) affects 6.8 million people worldwide and is characterized by alternating periods of remission and random relapse. People with IBD are also at higher risks of getting malnutrition and dehydration. To help maintain the physical and psychological well-being of IBD patients and reduce their burden, this project aims to develop a non-invasive, wearable device that is able to monitor and alarm for the risk of an IBD flare-up, as well as track the patients' nutrition and hydration status by sampling human sweat where abundant biomarkers including glucose,  $\text{Na}^+/\text{K}^+$  ions, C-reactive protein (CRP) and interleukin-1 $\beta$  (IL-1 $\beta$ ), are found to reflect rich physiological information. We constructed an early-stage proof-of-principle glucose sensor that could detect glucose levels under in vitro conditions accurately, demonstrated by a high Pearson correlation coefficient  $r = 0.99$  and various statistical analysis. A proof-of-principle signal processing circuit and a PC-based program were designed for complex signal conditioning and real-time wireless transmission. The combination of the work done serves as a base stone and sets a direction towards developing a wearable sweat-based device for IBD management. All codes used within the project can be found at <https://github.com/Roldbach/SweatDetection>.

## 1 Introduction

### 1.1 Motivation

Inflammatory Bowel Disease (IBD) is a disease that affects 300,000 UK citizens and 6.8 million people worldwide (data from 2017) [1]. It is characterized by chronic and recurrent inflammation, where the body's own immune cells attack the gastrointestinal tract. It is hypothesized that a combination of factors such as genetic susceptibility, a dysregulated immune system, and environmental factors, can result in the development of IBD [2]. Currently, medical treatment might help maintain remission and avoid disease progression. However, inflammation may persist and contribute to a risk of symptomatic and unpredictable relapses: these random attacks heavily disrupt the patient's physical and psychological well-being. Symptoms of IBD flare-ups include diarrhoea, fatigue, abdominal pain and rectal bleeding. Frequent bowel movements also cause dehydration and loss of nutrients, and more than half of 505 patients in a 2010 study reported having these flares  $\geq 1$  per week or month [3].

The gold standard tests for diagnosing IBD flare-ups are blood tests and stool samples, which are not convenient for patients, as they require them to regularly go into hospital. A monitoring device to predict

disease flares and their severity could thus significantly advance clinical practice: it would potentially allow gastroenterologist intervention to prevent flares by providing suitable medication to the patient as soon as there is suspicion a crisis might start. This would reduce the serious complications of severe flare-ups, which can lead to hospitalisation and bowel resection surgery if left untreated. This will, in the long term, reduce the burden of IBD on both patients and healthcare systems.

### 1.2 Background

#### 1.2.1 Viable Biomarkers for IBD Management

It has been reported that the level of cytokines in time and space orchestrates the development, recurrence, and exacerbation of the inflammatory process in IBD [4]. The inflammation-associated cytokines include IL-6, IL-1 $\beta$ , TNF- $\alpha$  and more. Research has shown that levels of interleukin 1 $\beta$  in IBD patients were higher and increased during flare-ups [5][6]. In addition to IL-1 $\beta$ , CRP, which is an acute-phase protein produced mainly by hepatocytes in response to a variety of acute and chronic inflammatory conditions, is also an inflammatory marker that correlates with disease activity of IBD, and is usually elevated in an IBD flare [7]. This led us to think about using interleukin 1 $\beta$  and CRP as biomarkers for tracking inflammation.

### **1.2.2 Nutrition and Hydration Status of IBD Patients**

Malnutrition and dehydration are common in IBD patients [8][9]. Several reasons are associated with malnutrition in patients with IBD: (1) The decrease of oral food intake due to symptoms of nausea, abdominal pain, vomiting, and diarrhoea during flare-ups or fasting/prolonged diets restriction required by hospitalization; (2) Malabsorption due to impaired epithelial transport and loss of integral epithelium, overgrowth of bacteria and frequent bowel movements; (3) Increased energy expenditure; (4) Medication; (5) Gastrointestinal nutrient loss by inflammatory diarrhoea [8]. Moreover, conditions such as gastrointestinal losses related to diarrhoea, reduced oral water intake (for alleviating abdominal pain), and decreased absorption of water due to the removal of a portion of the gastrointestinal tract are also the main reasons for dehydration [9]. Also, the patient's diet has been suggested as an environmental factor that triggers inflammations: maintaining a healthy diet might help progress in remission. Therefore, we thought tracking the nutritional and hydration status such that patients can adjust their diet, water intake, and therapeutic regimens adequately, would be important for preserving their health.

Although a full nutritional evaluation requires assessment of a variety of markers and involves different methods [8], and whether nutrition status is related to blood sugar level is not clear, we will attempt to estimate nutrition status by monitoring glucose levels, as they, to a certain extent, reflect the amount of food intake and quality of diet, and sweat glucose is reported to be metabolically related to blood glucose [10]. As for the hydration status assessment, it appears that many indices such as bioelectrical impedance, heart rate and blood pressure changes, levels of plasma osmolality and sodium concentration, and the blood urea/creatinine ratio are widely used [11]. Keeping track of sweat  $[K^+]$  and  $[Na^+]$  will be used as the way of monitoring dehydration in our project, as increased blood serum  $[Na^+]$  &  $[K^+]$ , and a significantly higher sweat  $[Na^+]$  were observed within dehydration status in a previous study [12].

### **1.2.3 Sweat as a Sampling Medium**

Our plan is to make a device that continuously monitors the risk of IBD recurrence. However, continuous monitoring of relevant biomarkers from samples such as blood and faeces is not really feasible in a comfortable or non-invasive way. A device that samples blood regularly, for example, would either require continuous access to blood or to regularly have to pierce blood vessels, which can damage the blood vessels. Using sweat as a sampling medium shows more promise, as it not only allows the device to be noninvasively brought into closest proximity to the

sample, but also allows it to be most convenient and ergonomic for the patients. We envision our device to be worn on the wrist, however, theoretically, the device could be placed anywhere on the skin, to the patients' preferences.

Sweat contains a range of analytes, including metabolites (e.g. glucose), ions (e.g. potassium and sodium ions), trace elements, and small amounts of large molecules [13]. Moreover, there has been promising research into the presence of biomarkers relating to IBD flares in eccrine human sweat [14][15]. *Cizza et al* [14] demonstrated that cytokines such as interleukin 1 $\beta$  in skin sweat are strongly correlated to that in the blood of patients with major depressive disorder (MDD). *Jagannath et al* [15] reported the presence and quantification of CRP in human eccrine sweat. Therefore, using sweat as a sampling medium for IBD management is seen as highly promising.

### **1.2.4 Recent Developments in Sweat-based Wearable Devices**

There are a plethora of sweat-based wearable biosensing devices that have already been developed for diverse applications using different innovative techniques [16]. For instance, advances have been made in developing a multiplexed, integrated, and miniaturized biosensor platform for in situ perspiration analysis, and improving wearability by incorporating flexible materials [17]. For its application in IBD management, a first proof-of-feasibility work of continuous IL-1 $\beta$  and CRP monitoring in passively expressed eccrine sweat, by using a wearable sensing platform for the purpose of tracking inflammation and warning in the event of an IBD flare-up, was done by *Jagannath et al* [18]. Our project was greatly inspired by the work described above.

## **1.3 Aims & Objectives**

We aim to develop a non-invasive, wearable device that is able to detect the levels of IL-1 $\beta$  and CRP in sweat in order to monitor the risk of an IBD flare-up. The device should also measure glucose and hydration levels in order to provide the user with a better picture of their overall health, as well as to avoid any deviation from normal levels, since IBD-associated symptoms can cause severe nutrient and water loss. If the device detects abnormal biomarker levels it should alert the patients of an increased risk of an IBD crisis, prompting them to seek their doctor or go to the hospital for further tests and advice. All in all, our device has the following objectives:

- To facilitate the flare-up detection process (making it effortless for the patient), to serve as an accurate crisis indicator, and to provide the patient with enough preparation time in case of an acute event.

- To assess the patient's health with its glucose and hydration detection capabilities.
- To offer continuous, real-time monitoring with its wearable form factor.
- To reduce the impact IBD has on patient's lives and healthcare systems.

## 2 Methods

### 2.1 Material

Platinum/Iridium wire was obtained from Advent Research Materials, USA. Silver wire and Gold wire were obtained from Goodfellow, UK. Epoxy resin was purchased from Robnor Resinlab Ltd, and alumina slurries were bought from Buehler, USA. Glucose oxidase (GOx, from Aspergillus niger) was obtained from Sekisui Diagnostics. Potassium chloride (KCl), ferrocene, poly(m-phenylenediamine) (mPD), phosphate buffered saline (PBS), glycerol, bovine serum albumin (BSA), poly(ethylene glycol) diglycidyl ether (PEG-DE), 3,4-ethylenedioxythiophene (EDOT), poly(sodium 4-styrenesulfonate) (Na-PSS), bis(2-ethylhexyl) sebacate (DOS), sodium ionophore X (Na ionophore X), potassium tetrakis(4-chlorophenyl) borate (K-TClPB), poly(vinyl chloride) (PVC), tetrahydrofuran (THF), potassium ionophore I (valinomycin), polyvinyl butyral resin BUTVAR B-98 (PVB), sodium chloride (NaCl) and methanol were obtained from Sigma-Aldrich. Artificial cerebrospinal fluid (aCSF) consisted of KCl (2.7mM), NaCl (147mM), calcium chloride dihydrate (1.2mM) and magnesium chloride (0.85mM).

### 2.2 Fabrication of Needle Electrodes

The fabrication process of needle electrodes is fully described in [3]. Briefly, a 50  $\mu\text{m}$  Teflon insulated platinum/iridium wire (Pt90/Ir10, PTFE coated, insulation thickness 12.5 $\mu\text{m}$ ) and a 50 $\mu\text{m}$  insulated silver wire (Polyester coated, insulation thickness 75 $\mu\text{m}$ ) were threaded through a 27G hypodermic needle for the glucose sensor, while a 125 $\mu\text{m}$  insulated gold wire (PTFE coated, insulation thickness 160 $\mu\text{m}$ ) was used for the ion-selective electrode. The internal space of the needle was filled by the epoxy resin to position the wires and avoid the short circuit between working and reference electrodes. After the epoxy resin had been completely hardened, the sharp end of the needle was then carefully polished into a flat surface using the sandpaper, followed by different Alumina slurries (1 $\mu\text{m}$ , 0.3 $\mu\text{m}$ , 0.05 $\mu\text{m}$ ). The silver wire was further chloridised to create a stable Ag/AgCl reference electrode by electropolymerisation using 1M KCl solution. The voltage was held at 0V for 20 seconds and then polarised to +0.45V for 15 minutes. For the glucose sensor only, the needle shaft was acting as the counter electrode. Figure 1 shows both type of sensors.

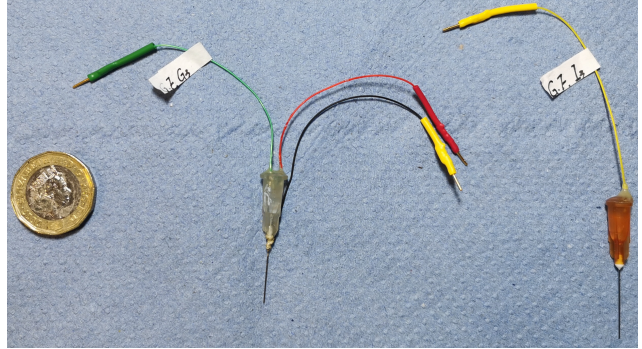


Figure 1: Needle Electrodes: Glucose Sensor (left), Ion-selective Sensor (right)

### 2.3 Preparation of Glucose Sensors

#### 2.3.1 Interference Membrane

The interference membrane was prepared by dissolving 108.14mg mPD into 10ml PBS (10mM, pH=7.4), which was further electropolymerised onto the working electrode. Similar to the chlorodisation, the voltage was held at 0V for 20 seconds and then polarised to +0.7V for 20 minutes. Finally, an extra holding at 0V for 5 minutes was necessary for the stabilisation of the membrane. This layer can efficiently protect the working electrode against interference from other untargeted electroactive species in the sweat.

#### 2.3.2 Enzyme Membrane

The enzyme membrane cocktail consisted of GOx (6% weight by weight, w/w), BSA (3% w/w), PEG-DE (1.3% w/w), glycerol (1% w/w) and PBS (10mM, pH=7.4, 97.7% w/w). Both BSA and PEG-DE facilitate the immobilization of the enzyme. The method to attach the membrane was taken and optimized from [4]. Briefly, the needle was dipped into the 5 $\mu\text{l}$  cocktail for 90 seconds and then placed in an oven at 55°C for 2 hours.

### 2.4 Preparation of Ion-selective Electrodes

#### 2.4.1 Ion-electron Transducer

We used the same ion-electron transducer inspired by [5] to reduce the voltage drift in the measurement. Briefly, the poly(3,4-ethylenedioxythiophene) (PEDOT:PSS) cocktail consisted of 0.1M Na-PSS and 0.01 EDOT in a 5ml aCSF solution. To deposit this membrane onto the working electrode, a galvanostatic electrochemical polymerization was performed, where 61.3125nA (0.5mA/cm<sup>2</sup>) was constantly applied to the electrode.

#### 2.4.2 Ion-selective Membrane

The Na<sup>+</sup> selective membrane solution contained Na ionophore X (1% w/w), K-TClPB (0.18% w/w), PVC (30.2% w/w) and DOS (68.7% w/w), while the K<sup>+</sup> selective membrane solution had exactly the same composition except for the use of valinomycin (1% w/w) instead of Na ionophore X. The membrane solution was

further dissolved into 4ml THF and left to evaporate overnight.

#### 2.4.3 PVB Membrane

The PVB membrane solution was prepared by dissolving 79.1mg PVB and 50mg NaCl into 1ml methanol followed by sonication for 30 minutes. The solution was sealed using parafilm and stored at 4°C until use. The membrane was deposited onto the reference electrode by dipping the needle into 4 $\mu$ l membrane solution for 5 seconds and put upside down to dry at room temperature. This could reduce the potential drift in the measurement.

### 2.5 Evaluation of Sensor Performance

#### 2.5.1 Cyclic Voltammetry

In order to evaluate the basic functionality of needle electrodes and the presence of different membranes, a cyclic voltammetry (CV) test from -100mV to 500mV (versus Ag/AgCl reference electrode) for one cycle at a scan rate of 10mV/s in the ferrocene (1.5mM) solution was performed. The shape of the plot and the actual peak measurements were then compared with the theoretical values.

#### 2.5.2 In Vitro Accuracy of Glucose Sensors

To evaluate the in vitro accuracy of glucose sensors, a calibration curve was constructed for each sensor by recording the corresponding current responses when adding glucose with known concentrations into the PBS solution (10ml, 10mM). A linear graph could be plotted by finding the line of best fit using those obtained responses. After establishing the calibration curve, various known concentrations from low to high level for glucose were added and the responses were recorded. The corresponding concentrations could be calculated using the calibration curve, which could be then used for statistical analyses in the next step.

#### 2.5.3 Statistical Analysis of Glucose Sensors

For each sensor, we performed a 2-sample Student's T test with a confidence interval (CI) of 95% to determine whether there is significant statistical difference between the measured concentrations and the input concentrations. Further more, Pearson Correlation and Bland-Altman test were also performed to determine whether the responses followed a strong linear relationship as expected.

## 2.6 Signal Processing and Transmission

#### 2.6.1 Design of Processing Circuits

Our design of processing circuits (Extended Data Figure 5) was strongly inspired by [5]. For amperometric signals which came from the glucose sensor, a transimpedance amplifier was used first to convert the current signals into voltage signals, which were simultaneously resolved so they could fit the analogue-to-digital converter later. As the transimpedance amplifier would

generate a negative voltage output, a voltage inverter was followed to ensure that the input of analogue-to-digital converter would be only positive. For proof-of-principle purpose, we used the gain mentioned in [5] directly (1M $\Omega$  for the glucose sensor) for simulation but this could be easily adjusted according to our own sensor operation range. Alongside this, the circuit included a low-pass filter, which could further reduce the interference from unwanted noise and facilitate the sensor calibration at the circuit level. We used OrCAD 17.02 to simulate the circuit where a DC sweep test was performed to check the linearity between the voltage output and the current input.

#### 2.6.2 Design of Arduino Circuit

The Arduino Uno Rev3 (Extended Data Figure 6) was chosen as the core circuit controller due to its low requirement of power and cost and its powerful functionality with the popular Arduino development environment. By using the built-in analogue-to-digital converter block and the capability to establish stable serial communication with the computer, the signals from various sensors could be transmitted to the Bluetooth transceiver after conditioned by the processing circuit. For proof-of-principle purpose, all signals except the temperature (measured by an external DHT temperature sensor module) were randomly generated by the built-in functions with reasonable ranges obtained from [5] for now, which could demonstrate the functionality of signal transmission and Bluetooth communication of the circuit. By using light-emitting diodes (LED) with different wavelength and a passive buzzer, an alarm could be fired with an ambulance-like effect when the command is received from the Bluetooth serve (computer).

#### 2.6.3 Implementation of Customized PC Program

A PC based lightweight program was written in Python, which could provide a user-friendly interface (Extended Data Figure 8) to the user as well as various functions. To enable the functionality of the program, the user need to manually pair the Arduino with the computer first. By clicking the start button, the program would automatically establish a secure Bluetooth connection to the Arduino, which could then start the real-time data processing and transmission without any other commands required. Besides this, the program is capable of plotting various graphs for those data against time with different time scales (last day/last week/last month) and automatically save them to the local storage. Additionally, the user could modify the setting according to their own requirements. Last but not the least, the built-in timer could check the health status of the user through the stored data periodically and send commands to the Arduino to fire the alarm if the health status is in danger. Extend Figure 7 displays the detailed class design of the program.

Test Condition	Response of Glucose Sensor (nA)					Ideal Response (nA)
	1	2	3	4	5	
Clean	10.74	10.54	9.34	9.92	11.9	8
After Chlorodisation	11.35	11.45	8.67	12.87	11.11	8
After mPD Coating	2.03	1.68	1.29	1.76	1.07	0

Test Condition	Response of Ion-Selective Electrode (nA)					Ideal Response (nA)
	1	2	3	4	5	
Clean	19.57	18.82	Overflow	18.83	19.65	20

Table 1: Anodic Peak Responses of Glucose Sensor & Ion-selective Electrode in CV under Different Conditions

### 3 Results & Discussion

#### 3.1 Evaluation of Basic Functionality of Needle Electrodes

To check the basic functionality and detect any short circuit within the electrodes, a CV test was performed and a globally right-shifted sigmoid plot was expected, which stayed at the anodic peak for a longer time compared with that at cathodic peak, due to the usage of the commercial Ag/AgCl reference electrode. The ideal anodic peak was about 8nA for the glucose sensor and 20nA for the ion-selective electrode, which was significantly related to the material of the electrode as well as the solution used for the test. It could be observed from (Figure 2a, 2b) and (Table 1) that all electrodes except ISE 3 could construct the expected shape with an acceptable bias in the anodic peak, serving as a good starting point for further steps.

#### 3.2 Evaluation of Chlorodisation of Glucose Sensors

After chlorodising the Ag reference electrode in the glucose sensor for a more stable performance, an evenly distributed sigmoid plot was expected with the same anodic peak. (Figure 2c) and (Table 1) could show that the results from all glucose sensors are in agreement with the ideal results, demonstrating the presence of Ag/AgCl reference electrode in the glucose electrodes.

#### 3.3 Demonstration of Presence of Interference Membrane

The interference membrane was electropolymerised onto the working electrode within the glucose sensors. A complete flat plot was expected from the CV test as the membrane could inhibit the redox reaction in the solution by blocking the diffusion of particles. From (Figure 2d) and (Table 1) it could be observed that almost no current was detected in the CV test for every glucose sensor, demonstrating the presence of interference membrane on the working electrodes. The bias might come from the sloped end of the needle shaft, which varied the effective sensing area and influenced the behaviour of the sensor. To tackle this problem, the sensor could be re-polished more carefully while keeping it perpendicular to the sand paper during the whole process.

#### 3.4 In Vitro Accuracy of Glucose Sensors

We evaluated the in vitro accuracy of glucose sensors by a constructing calibration plot separately and performed statistical analysis, where we collected 24 different responses in total. (Figure 3a and d) show the representative amperometric response of Glucose 4 and 5 in 0~0.6mM glucose solution. By using the first 10 responses, a strong linear calibration curve (Figure 3b and e) could be plotted within 0.2~1.8mM for each sensor, which could achieve a Pearson correlation coefficient  $r=0.997$  for Glucose 4 and  $r=0.995$  for Glucose 5. However, this significantly decreased to  $r=0.843$  for Glucose 4 and  $r=0.880$  for Glucose 5 when doing a 24-point calibration within 0.2~40mM. This might be due to the fact that the later responses exceeded the valid dynamic range of the glucose sensor, which was strongly determined by the composition of the membranes. The sensitivity was 0.770nA/mM for Glucose 4 and 0.548nA/mM for Glucose 5 respectively. Furthermore, by calibrating the sensor using randomly chosen 12 responses, a 2-sample Student's T test was performed with a p-value  $0.694>0.5$  for Glucose 4 and  $0.622>0.5$  for Glucose 5, demonstrating the reliability of the measurements of both sensors. Alongside this, the Bland Altman analysis (Figure 3c and f) was constructed by calibrating the sensor using the first 7 responses and comparing with the following 5 responses. It could also confirm the agreement between the measured results with the known input concentrations, with a mean bias of -0.01mM for Glucose 4 and -0.66mM for Glucose 5 respectively and all responses were with the  $\pm 1.96$  standard deviation interval.

#### 3.5 Demonstration of Presence of Ion-electron Transducer

The PEDOT:PSS membrane was deposited onto the working electrode of ion-selective electrodes by galvanostatic electrochemical polymerization to help the sensor maintain a high potential stability. Theoretically the reaction should be protected against oxygen as it could interfere the reaction and vary the property of the membrane. Surprisingly we successfully deposited the membrane without the usage of nitrogen. (Figure 2e) illustrated that the capacitance of the electrode was increased by showing a higher reaction cur-

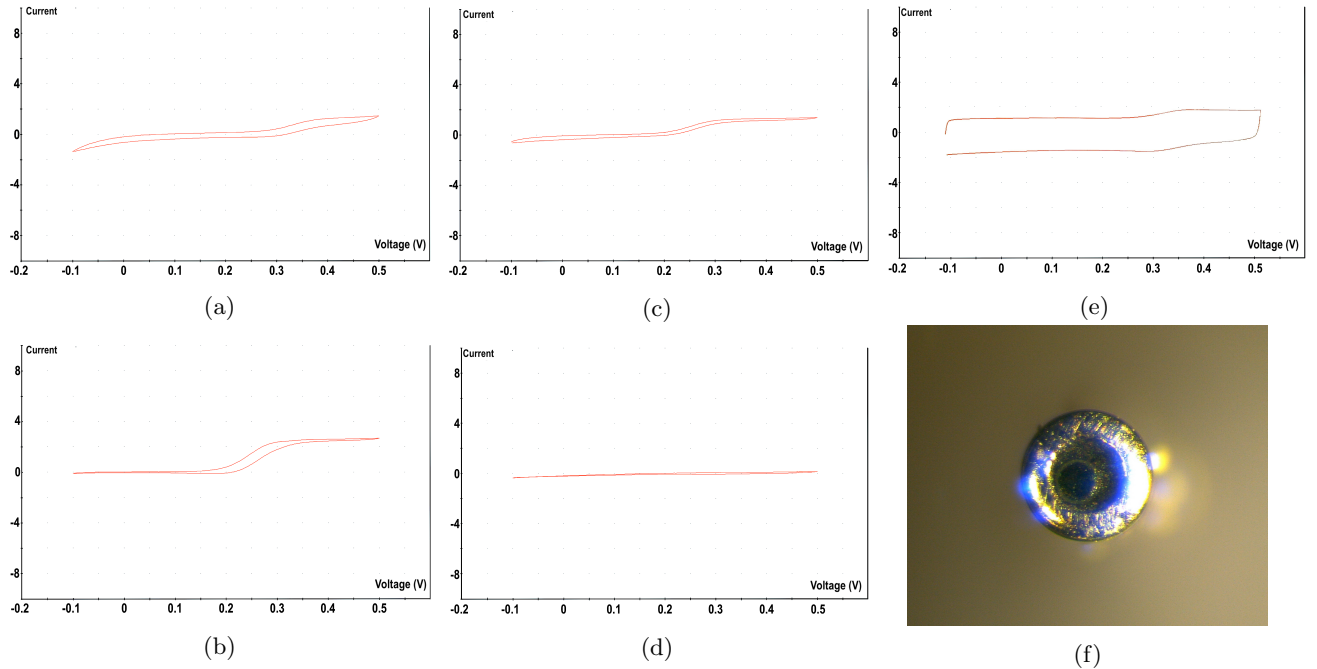


Figure 2: Results of cyclic voltammetry of electrodes under different conditions (a~e): (a) glucose sensor clean. (b) ion-selective electrode clean. (c) glucose sensor after chlorodisisation. (d) glucose sensor after mPD coating. (e) ion-selective electrode after PEDOT:PSS deposition and (f) photo of ion-selective electrode after PEDOT:PSS deposition under microscope.

rent in the CV test, demonstrating the functionality of the ion-electron transducer. Alongside this, from (Figure 2f) it could be clearly seen that there were attachments on the surface of the gold wire, which shown blue luster. This is another powerful proof of the presence of ion-electron transducer.

### 3.6 Simulation of Processing Circuit

A DC sweep test was performed and an linear relationship between the output and the input was expected. (Extended Data Figure 4) clearly illustrates that as current input increased linearly, the voltage output also followed a strong linear relationship, which could demonstrate the accurate and unique mapping between the detected concentration and the sensor response.

## 4 Weaknesses & Opportunities

Our current glucose sensor doesn't facilitate non-invasive detection due to its needle-based structure. We would need to further explore the possibility of a chip-based sensor, which would be more suitable for a wearable device. At the same time, the Arduino circuit was constructed based on a breadboard, which could be further integrated into a printed circuit board (PCB) as a more efficient design. Also, the monitoring program is only PC based which is very inconvenient for a wearable device. We could implement a mobile version for the daily use in the future.

Having proven the feasibility of continuous glucose

concentration detection in solution with needle-based glucose-sensing electrodes, the next step is to undergo this similar process for potassium and sodium ions sensors and extend the work into fabricating sensors for IL-1beta and CRP through the antibody affinity capture mechanism. The successful proof-of-principle of continuous cytokine, inflammatory marker, and ions concentration monitoring would allow us to make the multiplexed sensing platform required by our aims.

In order to ensure the reliability and accuracy of the sensors when in contact with human eccrine sweat, it would be important, at later stages, to perform sensor testing with human eccrine sweat. Moreover, after connecting every component of the device, further testing such as an on-body test would also be useful to assess the product's ability to monitor targeted biomarkers in sweat when worn by the user.

As the device is designed to be worn for extended periods of time, it is worth thinking about improving its wearability and comfortableness. For example, a flexible electrode substrate and a flexible circuit board may be used so that there is more mobility. A concept CAD design is shown in (Extended Data Figure 9).

Finally, if the product is to be brought into the market, according to the European MDR (Medical Device Regulation) rules, a clinical evaluation will need to be performed, technical documentation will need to be

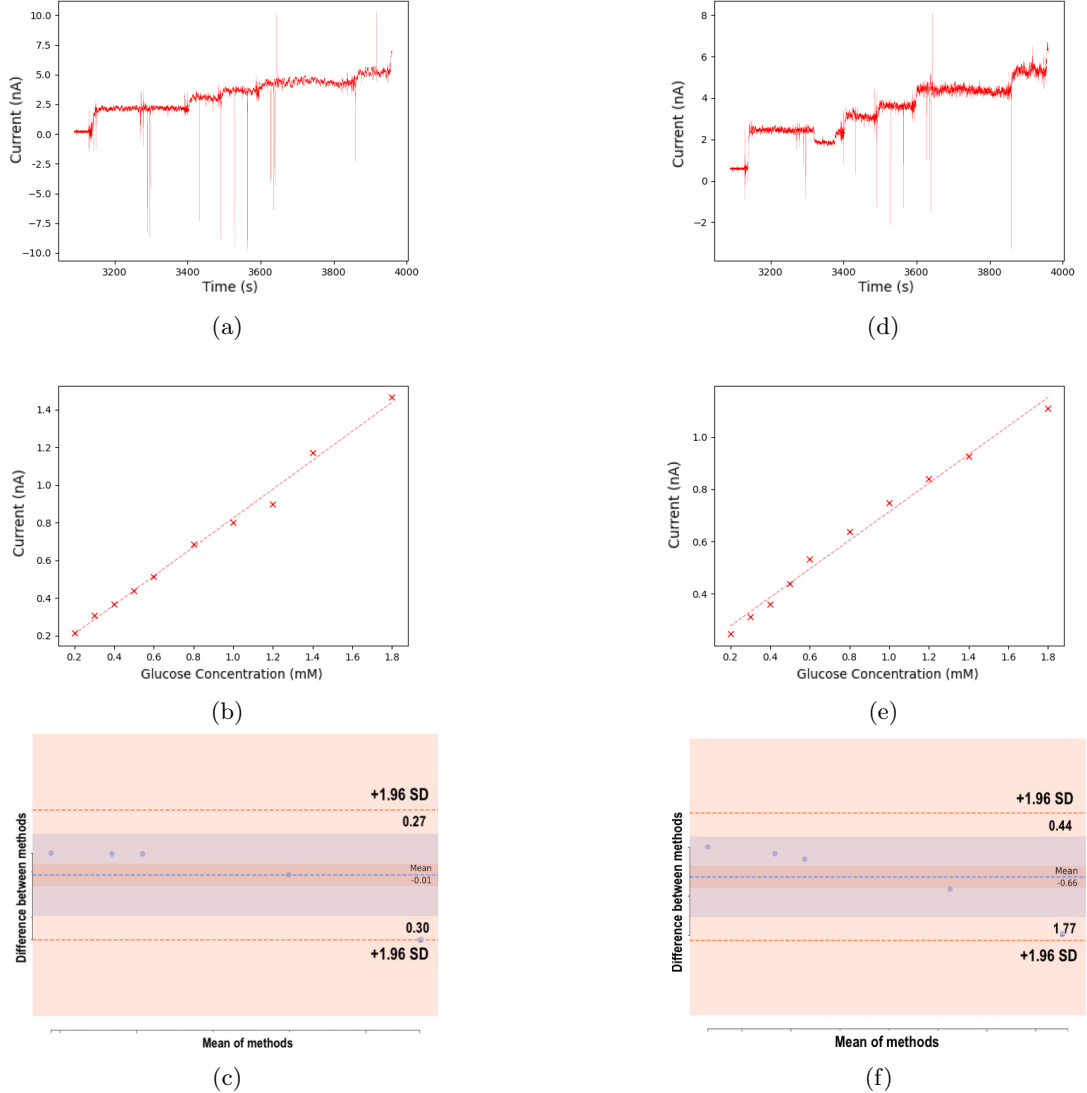


Figure 3: Experimental Characterization of Glucose Sensors: (a, d) current response of glucose 4, 5 respectively in PBS solution. (b, e) 10-point calibration curve of glucose 4, 5 respectively. (c, f) Bland-Altman Analysis of glucose sensor 4 and 5 respectively by first 7-point calibration

provided, and it will also need to undergo a conformity assessment process with the MDR [20]. Given the class tier (Class I) and the measuring functions in our device, we will also need to maintain a post-market surveillance report [20].

## 5 Conclusion

In summary, we constructed a proof-of-principle needle-based glucose sensor that could detect the concentration of glucose in the buffer solution continuously. This work could be further extended to the detection of biomarkers of IBD through the antibody affinity capture mechanism. The reliable and robust measurement was achieved by the attachment of the interference membrane as well as the use of stable Ag/AgCl reference. The performance of the glucose sensor was evaluated by plotting the calibration curve,

where a strong Pearson correlation coefficient and insignificant statistical evidence from the 2-sample Student's T test have demonstrated the reliability and accuracy of our measurements taken from the in vitro buffer solution. Besides this, we also came up with a proof-of-principle circuit inspired by [5], which could analyze and process the raw data from the sensor, and a PC based program, which allows the real-time signal transmission and displays signals to the user in a clearer way. With an external Arduino circuit, the alarm could be fired when the health status of the user is in danger. These are the base stones of the bridge that could connect the detection of biomarkers from the sensor with the complex signal processing, transmission and displaying, which in turn make the fully integrated wearable device possible.

## 6 Extended Data

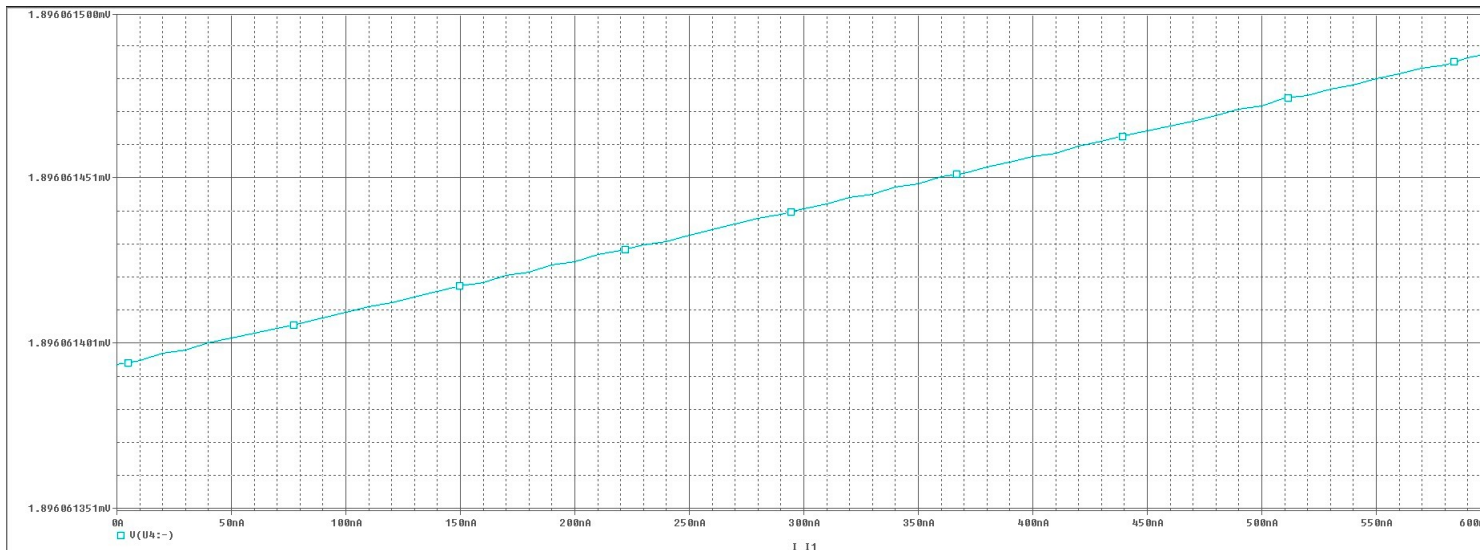


Figure 4: Simulation of Glucose Sensor Processing Circuit in a DC Sweep Test

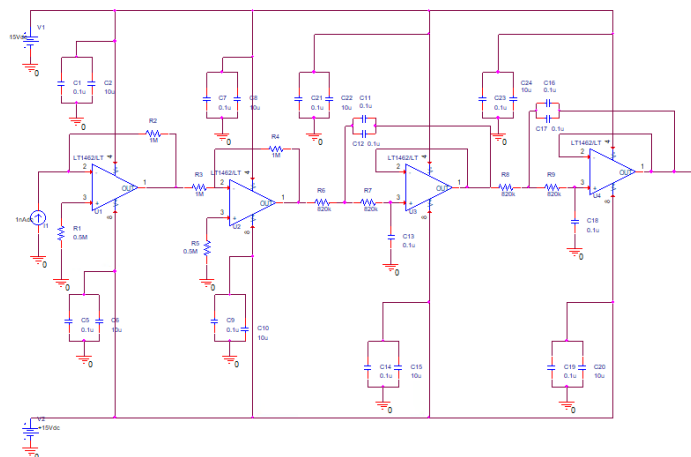


Figure 5: Circuit Schematic of Glucose Sensor Processing Circuit

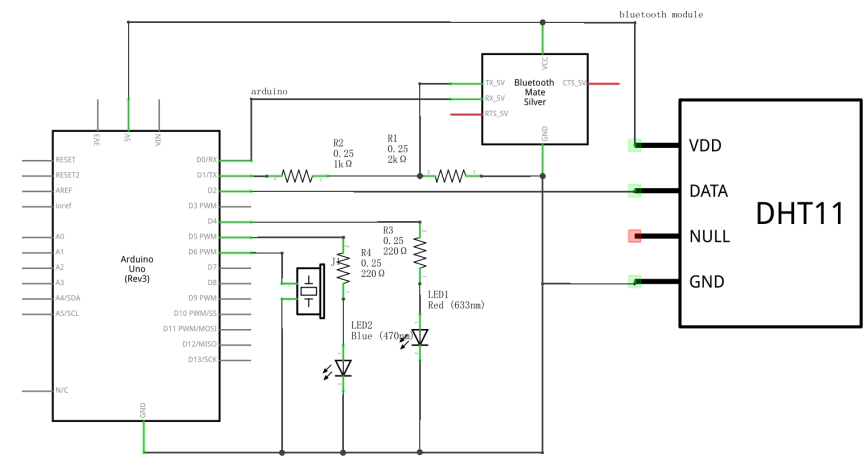
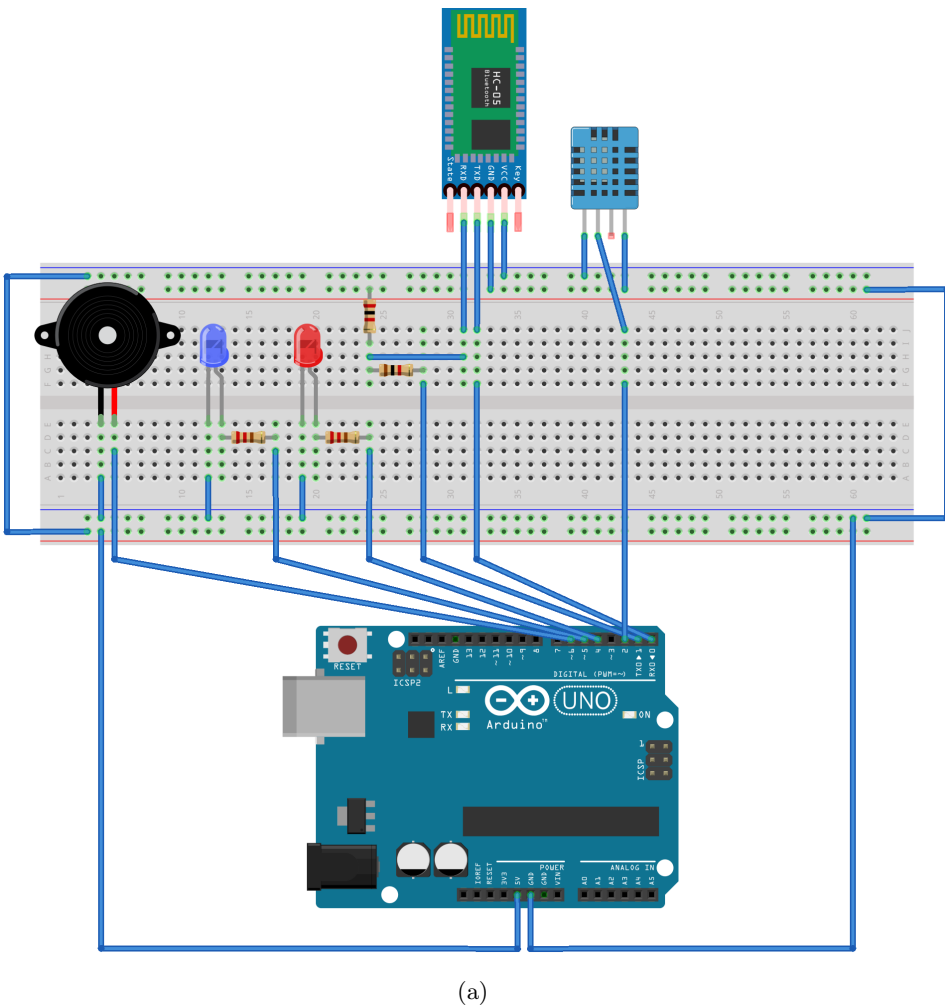


Figure 6: Arduino Circuit: (a) breadboard schematic of Arduino circuit.  
 (b) schematic of Arduino circuit.

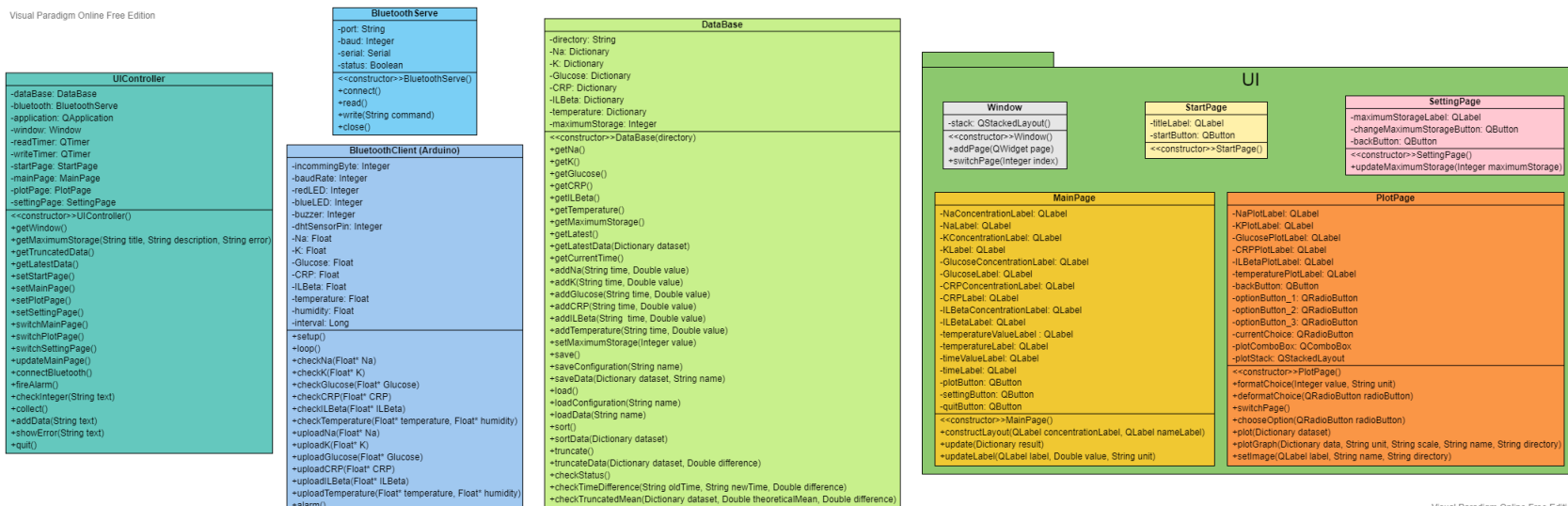


Figure 7: Class Diagram of Sweat Monitoring Program

13

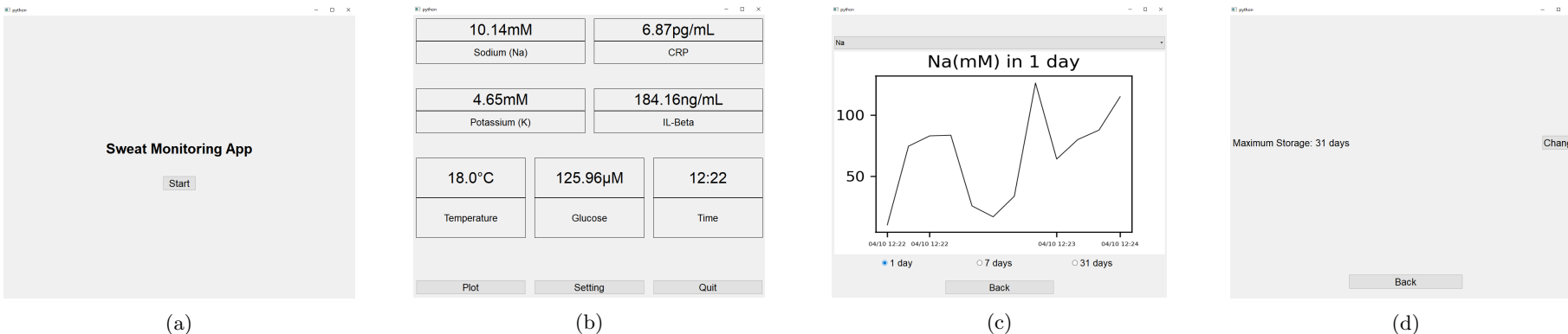


Figure 8: The Customized PC based Program: (a) start page of the program, which allows the user to connect to the Bluetooth module. (b) main page of the program, which displays real-time levels of biomarkers within the sweat. (c) plot page of the program, which illustrates the general health status in a certain time scale. (d) setting page of the program, which allows the user to modify the setting of the program,

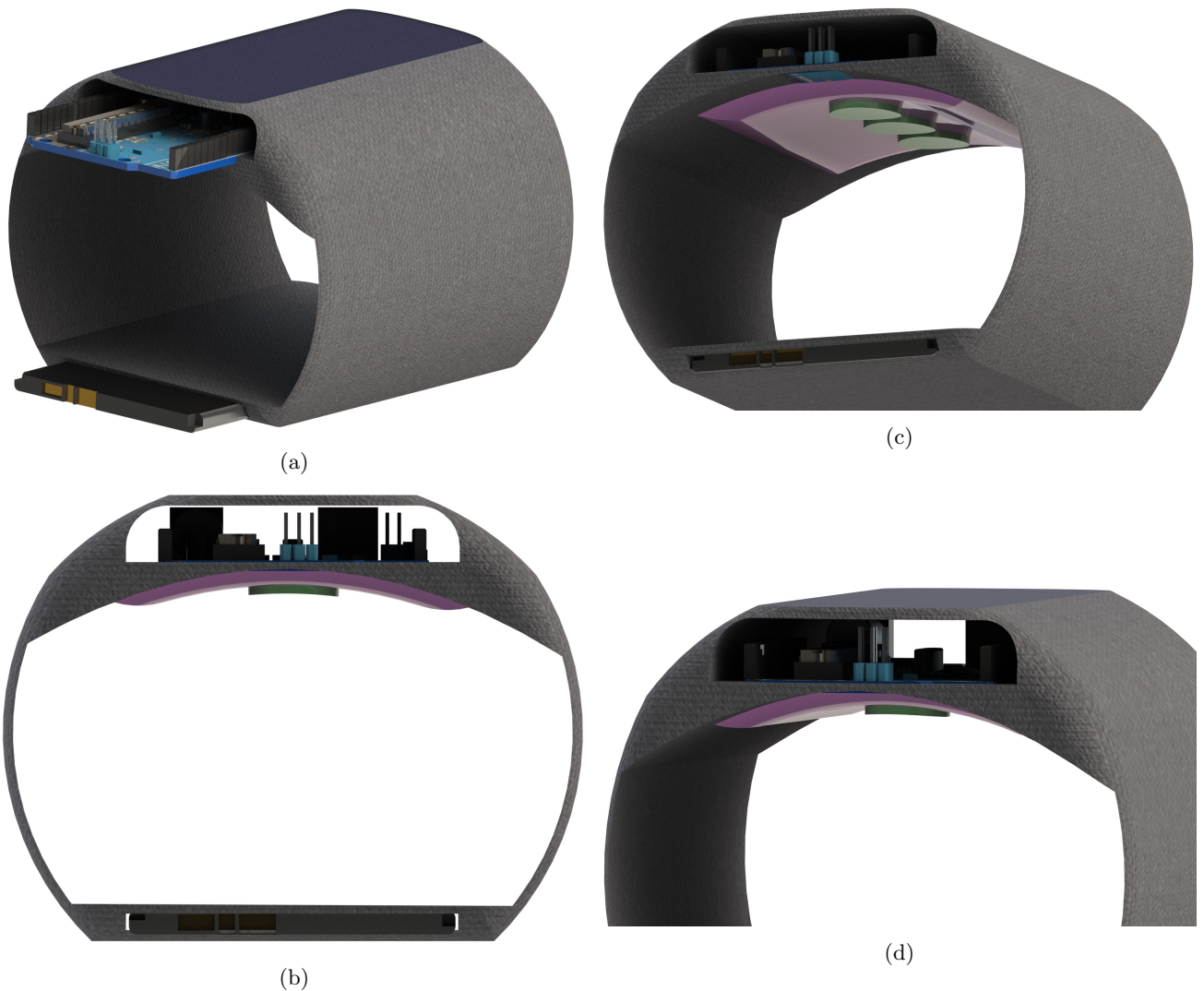


Figure 9: Concept Design of Wearable Device: An Arduino UNO is housed within an armband form-factor, and connected to a flexible sensor array (in purple), all powered by a removable battery (a) isometric view of the device. (b) side view of the device. (c) bottom view of the device. (d) front view of the device. All holes would be sealed.

## 7 References

- [1] GBD 2017 Inflammatory Bowel Disease Collaborators. (2019) The global, regional, and national burden of inflammatory bowel disease in 195 countries and territories, 1990–2017: a systematic analysis for the Global Burden of Disease Study 2017. *The Lancet*. Volume 5, Issue 1. doi: 10.1016/S2468-1253(19)30333-4
- [2] Baumgart, D. and Carding, S. (2007) Inflammatory bowel disease: cause and immunobiology. *The Lancet*. 369(9573), 1627-1640. doi: 10.1016/s0140-6736(07)60750-8
- [3] Susan C. Bolge, Heidi Waters, Catherine Tak. (2010) Self-reported frequency and severity of disease flares, disease perception, and flare treatments in patients with ulcerative colitis: results of a national internet-based survey. *National Institutes of Health*. 32(2), 238-45. doi: Piech10.1016/j.clinthera.2010.02.010
- [4] Sanchez-Muñoz, F., Dominguez-Lopez, A. and Yamamoto-Furusho, J. (2008) Role of cytokines in inflammatory bowel disease. *World Journal of Gastroenterology*, 14(27), 4280. doi: 10.3748/wjg.14.4280
- [5] Reimund, J., Wittersheim, C., Dumont, S., Muller, C., Baumann, R., Poindron, P. and Duclos, B. (1996) Mucosal inflammatory cytokine production by intestinal biopsies in patients with ulcerative colitis and Crohn's disease. *Journal of Clinical Immunology*, 16(3), 144-150. doi: 10.1007/bf01540912
- [6] Vounotrypidis, P., Kouklakis, G., Anagnostopoulos, K., Zezos, P., Polychronidis, A., Maltezos, E., Efremidou, E., Pitiakoudis, M. and Lyratzopoulos, N. (2013) Interleukin-1 associations in inflammatory bowel disease and the enteropathic seronegative spondylarthritis. *Autoimmunity Highlights*, 4(3), 87-94. doi: 10.1007/s13317-013-0049-4
- [7] Vermeire, S. (2006) Laboratory markers in IBD: useful, magic, or unnecessary toys?. *Gut*, 55(3), 426-431. doi: 10.1136/gut.2005.069476
- [8] Scaldaferrri, F., Pizzoferrato, M., Lopetuso, L., Musca, T., Ingravalle, F., Sicignano, L., Mentella, M., Miggiano, G., Mele, M., Gaetani, E., Graziani, C., Petito, V., Cammarota, G., Marzetti, E., Martone, A., Landi, F. and Gasbarrini, A. (2017) Nutrition and IBD: Malnutrition and/or Sarcopenia? A Practical Guide. *Gastroenterology Research and Practice*, 2017, 1-11. doi: 10.1155/2017/8646495
- [9] Phillips, Q. and Sanjai Sinha, M. (2022) Why It's Important to Stay Hydrated if You Have Crohn's. [online] EverydayHealth.com. Available at: <https://www.everydayhealth.com/crohns-disease/why-its-important-to-stay-hydrated-if-you-have-crohns/> [Accessed 9 April 2022].
- [10] Talary, M., Dewarrat, F., Huber, D. and Caduff, A. (2007) In vivo life sign application of dielectric spectroscopy and non-invasive glucose monitoring. *Journal of Non-Crystalline Solids*, 353(47-51), 4515-4517. doi: 10.1016/j.jnoncrysol.2007.03.038
- [11] Kavouras, S. (2002) Assessing hydration status. *Current Opinion in Clinical Nutrition and Metabolic Care*, 5(5), 519-524. doi: 10.1097/00075197-200209000-00010
- [12] Morgan, R., Patterson, M. and Nimmo, M. (2004) Acute effects of dehydration on sweat composition in men during prolonged exercise in the heat. *Acta Physiologica Scandinavica*, 182(1), 37-43. doi: 10.1111/j.1365-201x.2004.01305.x
- [13] Sonner, Z., Wilder, E., Heikenfeld, J., Kasting, G., Beyette, F., Swaile, D., Sherman, F., Joyce, J., Hagen, J., Kelley-Loughnane, N. and Naik, R. (2015) The microfluidics of the eccrine sweat gland, including biomarker partitioning, transport, and biosensing implications. *Biomicrofluidics*, 9(3), 031301. doi: 10.1063/1.4921039
- [14] Cizza, G., Marques, A., Eskandari, F., Christie, I., Torvik, S., Silverman, M., Phillips, T. and Sternberg, E. (2008) Elevated Neuroimmune Biomarkers in Sweat Patches and Plasma of Premenopausal Women with Major Depressive Disorder in Remission: The POWER Study. *Biological Psychiatry*, 64(10), 907-911. doi: 10.1016/j.biopsych.2008.05.035

- [15] Jagannath, B., Lin, K., Pali, M., Sankhala, D., Muthukumar, S. and Prasad, S. (2020). A Sweat-based Wearable Enabling Technology for Real-time Monitoring of IL-1 $\beta$  and CRP as Potential Markers for Inflammatory Bowel Disease. *Inflammatory Bowel Diseases*, 26(10), 1533-1542. doi: 10.1093/ibd/izaa191
- [16] Kim, J., Campbell, A., de Ávila, B. and Wang, J. (2019) Wearable biosensors for healthcare monitoring. *Nature Biotechnology*, 37(4), 389-406. doi: 10.1038/s41587-019-0045-y
- [17] Wei Gao, Sam Emaminejad, Hnin Yin Yin Nyein, Samyuktha Challa, Kevin Chen, Austin Peck, Hossain M. Fahad, Hiroki Ota, Hiroshi Shiraki, Daisuke Kiriya, Der-Hsien Lien, George A. Brooks, Ronald W. Davis Ali Javey. (2016) Fully integrated wearable sensor arrays for multiplexed *in situ* perspiration analysis. *Nature*. 529, 509–514. doi: 10.1038/nature16521
- [18] Sally A. N. Gowlers, Michelle L. Rogers, Marsilea A. Booth, Chi L. Leong, Isabelle C. Samper, Tonghathai Phairatana, Sharon L. Jewell, Clemens Pahl, Anthony J. Strong, Martyn G. Boutelle. (2019) Clinical translation of microfluidic sensor devices: focus on calibration and analytical robustness. *The Royal Society of Chemistry 2019*. 19, 2537-2548. doi: 10.1039/C9LC00400A
- [19] Natalia Vasylieva, Bogdan Barnych, Anne Meiller, Caroline Maucler, Loredano Pollegioni, Jian-Sheng Lin, Daniel Barbier, Stéphane Marinesco. (2011) Covalent enzyme immobilization by poly(ethylene glycol) diglycidyl ether (PEGDE) for microelectrode biosensor preparation. *Biosensors and Bioelectronics*. Volume 26, Issue 10, 3993-4000. doi: 10.1016/j.bios.2011.03.012
- [20] Ec.europa.eu. 2022. MDCG 2021-24 Guidance on classification of medical devices. [online] Available at: [https://ec.europa.eu/health/system/files/2021-10/mdcg\\_2021-24\\_en\\_0.pdf](https://ec.europa.eu/health/system/files/2021-10/mdcg_2021-24_en_0.pdf) [Accessed 10 April 2022].

## 7.1 Management Assessment

Our initial project planning, as laid out in the project pitch's Gantt Chart (Figure 10), turned out to be a little demanding. Although we carefully thought on who would be best to tackle each task, and our priority ordering made sense, we did not take into account certain delays we ended up facing, although we always left some runway time. This ended up happening especially with lab-related work, where our ideal start-date differed significantly from the one at which we actually were able to start, pushing our testing and results to the very limit date-wise. To a lesser extent, something similar happened with the app development, were we faced a last-minute change of programming language (from Java to Python, due to the graphing features) which would have made us save time had we thought about it earlier. Furthermore, we have had to tweak the "who-does-what" on-the-go, as we all follow separate career pathways with different deadlines, and we have each come to and left the UK at different dates due to COVID-19 restrictions. Thus, we have had to re-accommodate tasks based on everyone's availability. During the past 6 months, however, there are some important project management lessons we have learnt:

- **The importance of sub-division:** At the start, we found that if we did not divide the research/work, there would be a lot of overlap, and we would not be seizing our time the most efficiently. Wanting to change this, we were able to identify the key areas that form our project. This was mostly due to the mind-map we developed, which made us look at it from a structural perspective. Recognising these areas allowed us to divide into sub-groups and tackle each problem individually and simultaneously. This has made for efficient research and has allowed everyone to share their findings/thoughts on our regular meetings, as we have each become knowledgeable in our specific topic.
- **Little by little, the bird makes its nest:** Throughout the project, we have also taken a step-by-step approach. Rather than focusing on, say, designing and manufacturing the wearable device right from the start, we have focused on getting the sensors to work beforehand: first and foremost, we wanted a functional product. Realising this has made us work following a logical timeline, prioritising objectives, and setting small & achievable targets. Having short deadlines (typically weekly) has become a great way of measuring our progress and making the most out of our time. We have also recorded the key takeaways of every supervisor meeting we have had and have kept a record of everyone's research in separate folders, something we now, a few months later, really appreciate.
- **Communication & trust:** We have kept a unified approach towards communication between members from the start, that is, to openly update each other on the progress of the respective parts. Not only delivering in our individual parts, but also knowing how others are doing with theirs is crucial for (1) keeping up to pace with the whole project and (2) spotting potential risks. In our planning, we have always left runway time for each section, in case of unforeseen circumstances needed to be contained, which we have always flagged if spotted. This has helped the project to be mostly delivering on-time. Open communication has also helped build trust between us, a trait we deem essential in professional teamwork scenarios. At certain points, knowing we could rely on someone else has proven to be very helpful, and is the basis of good cooperation.

## Non-invasive Sweat Detection

Group Fantastic Detector  
Supervisor: Professor Bouteille

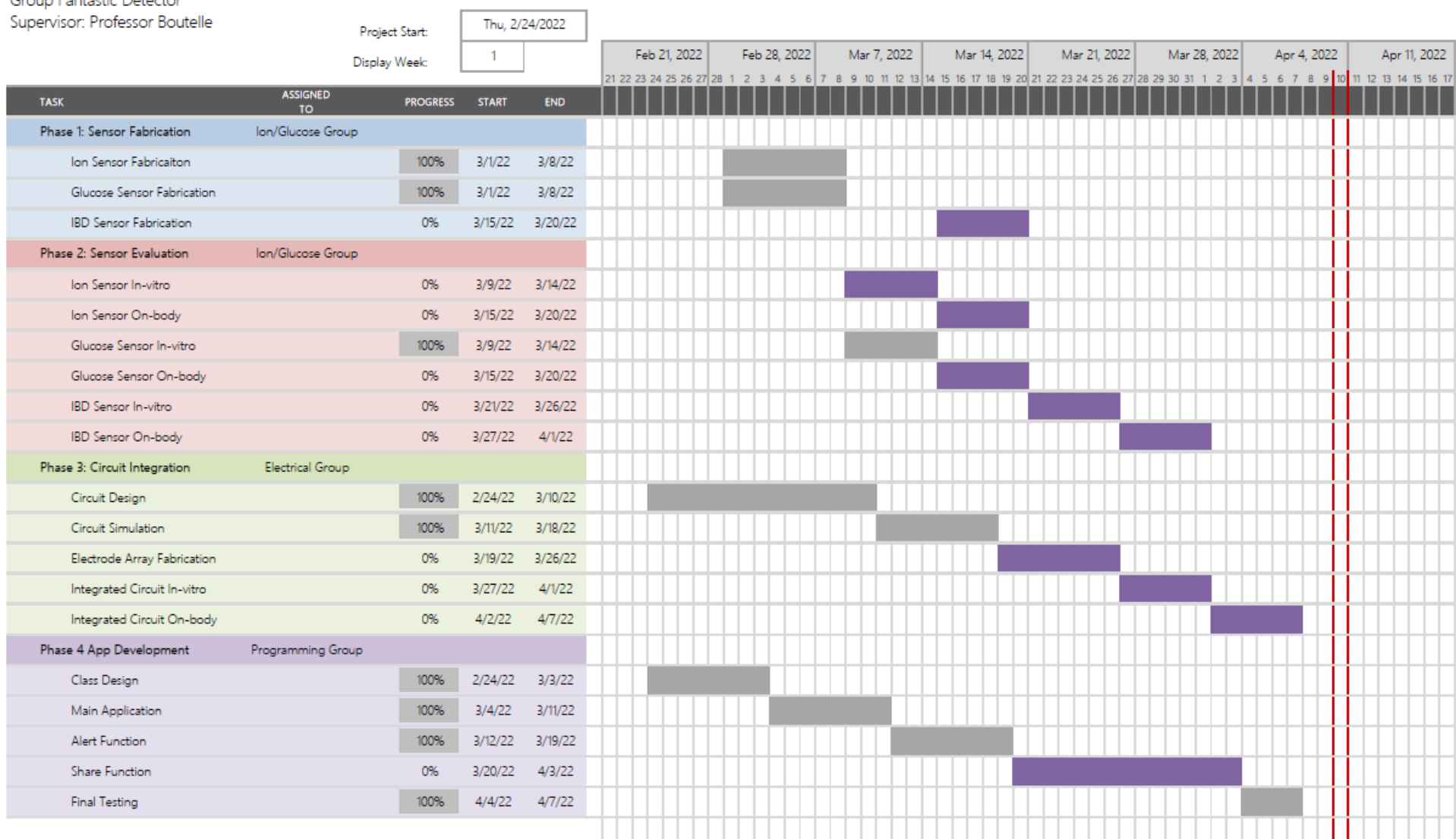


Figure 10: Gantt Chart of the Project